Amyolid precursor protein mediates presynaptic localization and activity of the high-affinity choline transporter

Baiping Wang*, Li Yang*, Zilai Wang*†, and Hui Zheng*†‡

*Huffington Center on Aging and †Department of Molecular and Human Genetics, Baylor College of Medicine, Houston, TX 77030

Edited by Xiaodong Wang, University of Texas Southwestern Medical Center, Dallas, TX, and approved July 17, 2007 (received for review May 2, 2007)

The key pathological features of Alzheimer's disease include synaptic dysfunction, profound changes in the cholinergic system, and deposition of β-amyloid peptides generated by proteolytic processing of the amyloid-β precursor protein (APP). However, the pathways linking APP with synaptic activity and cholinergic neuronal function are poorly understood. We report here that APP is essential in regulating the presynaptic expression and activity of the high-affinity choline transporter (CHT), a molecule that mediates the rate-limiting step of cholinergic synaptic transmission in both the neuromuscular junction and central cholinergic neurons. Loss of APP leads to aberrant localization of CHT at the neuromuscular synapses and reduced CHT activity at cholinergic projections. At the cellular level, we show that APP and CHT can be found in Rab5-positive endosomal compartments and that APP affects CHT endocytosis. Furthermore, we demonstrate that APP interacts with CHT through the C-terminal domain, providing support for a specific and direct regulation of CHT by APP through protein–protein interactions. These results identify a physiological activity of APP in cholinergic neurons, and our data indicate that deregulation of APP function may contribute to cholinergic impairment and AD pathogenesis.

neuromuscular synapse | Alzheimer's disease | cholinergic neurons | knockout mice | endocytosis

Genetic and biochemical evidence establishes a pivotal role of the amyloid-β precursor protein (APP) in Alzheimer's disease (AD) pathogenesis. APP processing generates β-amyloid (Aβ) peptides, which are deposited as amyloid plaques in the brains of affected individuals; point mutations or gene duplications of APP are causal for a subset of early onset familial AD (1, 2). APP is a member of a family of conserved type I membrane proteins with three mammalian homologs: APP, APP-like protein 1 (APLP1), and APLP2 (3). APP is highly expressed in neurons, where it has been shown to localize to postsynaptic densities, axons, and dendrites (4, 5). APP undergoes rapid anterograde transport (6–9) and is targeted to the synaptic sites of both the CNS and the peripheral nervous system. Despite the extensive studies on APP expression and processing, the physiological function of APP remains speculative and controversial (3).

Besides the amyloid pathology, AD is correlated with synaptic dysfunction and is recognized by profound changes in the cholinergic system. These changes include the loss of basal forebrain cholinergic neurons and impaired cholinergic innervation to the cortex and hippocampus, areas that have been implicated in memory, learning, and attention (10–12). Acetylcholine (ACh) is the neurotransmitter for central and peripheral cholinergic synapses, and the latter includes the mammalian neuromuscular junction (NMJ). ACh is synthesized by choline acetyltransferase (Chat) and packaged to synaptic vesicles by vesicular acetylcholine transporter (VaChT). ACh released from presynaptic terminals binds to acetylcholine receptors (AChRs) to elicit postsynaptic responses. However, the majority of ACh is quickly hydrolyzed by acetylcholinesterase to choline. The high-affinity choline transporter (CHT) recycles choline from the synaptic cleft back to the presynaptic terminals for ACh resynthesis (13). Of the orchestrated events leading to the regulation of ACh release and cholinergic neurotransmission, the rate-limiting step is the recycling of choline by CHT. Indeed, CHT capacity is considered a marker for the status of cholinergic transmission (13). In the presynaptic terminals, CHT has been shown to predominantly localize to synaptic vesicles and also can be found in endosomes (14, 15). The intracellular pool of CHT undergoes activity-dependent trafficking to the synaptic plasma membrane (PM) (14), which can then be internalized by clathrin-mediated endocytosis (15, 16). As such, the membrane CHT concentration is likely controlled by membrane trafficking and endocytosis, the balance of which critically mediates CHT membrane capacity and cholinergic neurotransmission.

We report here that the APP family of proteins represents a class of molecules that mediates the posttranslational regulation of CHT activity in both the NMJ and central cholinergic neurons. We provide biochemical data to support a role for APP in regulating CHT endocytosis through physical interactions of the two proteins.

Results

CHT Fails to Localize to Presynaptic Terminals of *APP/APLP2*-Null NMJ. The mammalian NMJ is a highly specialized synaptic structure in which the presynaptic terminals of motor neuron axons are closely apposed to postsynaptic AChRs of the muscle fiber (17). We demonstrated diffused pre- and postsynaptic structures and excessive nerve sprouting in NMJs of mice doubly deficient in *APP* and *APLP2* [*APP*/*APLP2* or double knockout (dKO)] (18). Because CHT is the rate-limiting step in ACh synthesis and synaptic transmission, and because mice deficient in *CHT* exhibit similar NMJ defects, compared with *APP*/*APLP2*-null animals (19), we examined the localization of CHT in NMJs of *APP*/*APLP2*-null mice at the newborn [postnatal day 0 (P0)] stage when presynaptic abnormality was readily detectable. The littermate *APLP2* single-null animals (APLP2$^{-/-}$), generated by intercrossing mice heterozygous for *APP* and homozygous-null for *APLP2*, were used as controls because we did not identify overt morphological defects in these animals (18).

Author contributions: B.W., L.Y., and H.Z. designed research; B.W., L.Y., Z.W., and H.Z. performed research; B.W. and L.Y. contributed new reagents/analytic tools; B.W., L.Y., Z.W., and H.Z. analyzed data; and B.W., L.Y., and H.Z. wrote the paper.

The authors declare no conflict of interest.

This article is a PNAS Direct Submission.

Abbreviations: α-BTX, α-bungarotoxin; Aβ, β-amyloid; Ach, acetylcholine; AChR, acetylcholine receptor; AD, Alzheimer's disease; APP, amyloid-β precursor protein; APLP1, amyloid precursor-like protein 1; Chat, choline acetyltransferase; CHT, high-affinity choline transporter; CTF, C-terminal fragment; dKO, double knockout; HACU, high-affinity choline uptake; NMJ, neuromuscular junction; PM, plasma membrane; P*n*, postnatal day *n*; VaCHT, vesicular acetylcholine transporter.

‡To whom correspondence should be addressed. E-mail: huiz@bcm.edu.

This article contains supporting information online at www.pnas.org/cgi/content/full/0704070104/DC1.

In control NMJ, CHT was predominantly localized to presynaptic terminals and was closely apposed by the postsynaptic AChRs marked by α-bungarotoxin (α-BTX) labeling (Fig. 1*Aa–Ac*). Strikingly, in NMJs of *APP/APLP2* dKO animals, CHT immunoreactivity was almost exclusively localized to motor neuron axon branches and was barely detectable at synaptic sites (Fig. 1 *Ad–Af* and *C*). This finding is in sharp contrast to that of synaptophysin, which showed clear staining at presynaptic terminals despite a reduced overall coverage with postsynaptic AChR [supporting information (SI) Fig. 6*A*]. Because CHT has been shown to localize to a subset of synaptic vesicles that also were positive for VaChT (14), we performed immunostaining by using an anti-VaChT antibody to assess whether similar mislocalization could be seen with VaChT (Fig. 1*B*). We found no significant difference in the localization or density of VaChT at synaptic sites between *APLP2*-null control and *APP/APLP2* dKO mice (Fig. 1 *B* and *C*). Finally, to investigate whether the CHT defect in *APP/APLP2*-null animals could be secondary to defective synaptic transmission and/or nerve sprouting, we examined CHT localization in *Chat* KO mutants, which exhibit complete absence of ACh synthesis and release and excessive nerve sprouting (20). We detected normal expression of CHT in *Chat*-null mice, compared with the littermate wild-type controls (Fig. 1*D*). Double staining and quantification of CHT- and Chat-positive spinal cord motor neurons revealed normal number (SI Fig. 6*B*), morphology, and staining patterns between *APP/APLP2*-null mutants and the controls (data not shown). Coimmunostaining with anti-neurofilament and anti-CHT antibodies also failed to detect any accumulation of CHT in main nerve bundles of *APP/APLP2* dKO mutants (data not shown). Combined, these results strongly suggest that the APP family of proteins specifically and critically regulates the localization of CHT at presynaptic terminals of NMJ.

Aberrant Presynaptic Localization of CHT at Developing and Mature *APP*-Null NMJ. Our previous studies using general presynaptic markers did not identify appreciable morphological differences in *APP*-null NMJs, compared with wild-type controls (18). The severe impairment of CHT in *APP/APLP2* dKO mice prompted us to reexamine the *APP*-null NMJ using CHT as a presynaptic marker. We stained whole-mounts diaphragm muscles of P0 *APP*-null and littermate wild-type controls for CHT (Fig. 2*A*) and observed aberrant distribution of CHT in axon branches and an ≈38% reduction of CHT intensity in presynaptic terminals of *APP*-null NMJs. This finding is in contrast to synaptophysin or VaChT staining, which showed normal localizations in the *APP*-null NMJ (SI Fig. 7).

At P0, each synapse is innervated by multiple axonal terminals. These nerve terminals undergo an apparently asynchronous elimination process during postnatal development, and by P14, the NMJ becomes mature and singly innervated (21). Having established a clear CHT abnormality at the developing NMJ of *APP*-null mice, we went on to evaluate whether the phenotype persists to adulthood by performing triple labeling of CHT, synaptophysin, and α-BTX of P18 sternomastoid muscles of *APP*-null and wild-type controls (Fig. 2*B*). Reduced CHT staining was readily detectable in the *APP*-null NMJ, compared with the wild-type controls (Fig. 2 *Ba* vs. *Bd*). In contrast, staining with anti-synaptophysin antibody documented well formed neuromuscular synapses indistinguishable from the controls (Fig. 2 *Bb* vs. *Be*). Interestingly, although apparently normal CHT staining could be detected in the *APP*-null NMJ (Fig. 2*B*, open arrow), a subset of the synapses showed sparse CHT immunoreactivity (Fig. 2*B*, arrowheads). Analysis of 60 synapses from three *APP* KO mutants showed that ≈30% of the endplates exhibited reduced CHT coverage.

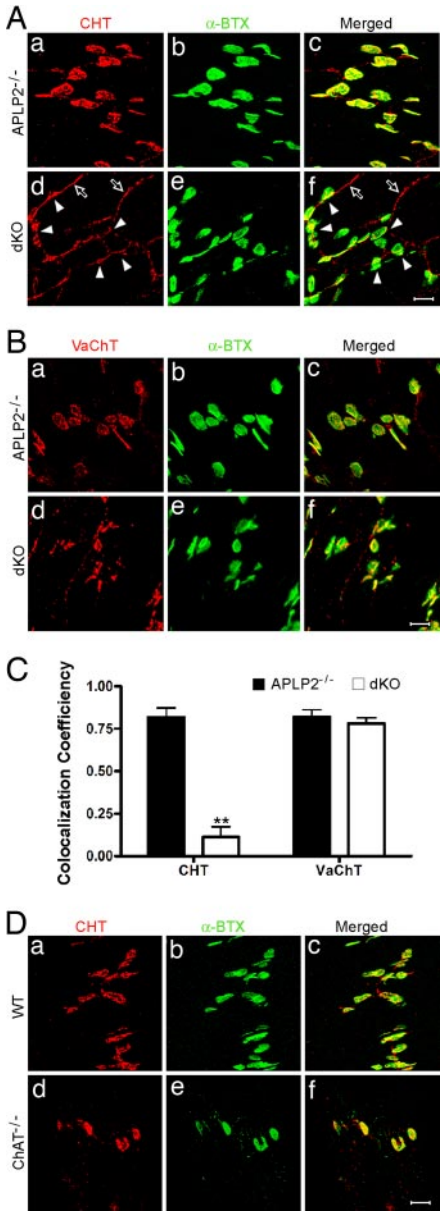

Fig. 1. Absence of CHT in presynaptic terminals of the *APP/APLP2*-null NMJ. (*A* and *B*) Whole-mount diaphragm muscles from P0 *APP/APLP2* dKO mice and littermate *APLP2*-null (APLP2$^{-/-}$) controls were stained with anti-CHT (*A*) or anti-VaChT (*B*) antibodies. AChR-positive postsynaptic endplates were labeled with Alexa Fluor 488-conjugated α-BTX. Open arrows in *A* mark the CHT staining beyond endplates, and representative synaptic sites are highlighted by the arrowheads. The images were captured by a confocal microscope and displayed as either individual staining or merged (last columns). (*C*) Quantification of the percentage of AChR-positive endplates covered by CHT or VaChT immunoreactivity (average ± SEM of 20 endplates per genotype). **, $P < 0.01$ (*t* test). (*D*) Double labeling of diaphragm muscles from the embryonic day 18 wild-type (WT) and *Chat* KO (Chat$^{-/-}$) mutant with the anti-CHT antibody (CHT) and α-BTX. (Scale bars: 20 μM.)

Diminished High-Affinity Choline Uptake (HACU) in *APP* and *APP/APLP2*-Null Brain Synaptosomes. Having established a structural and functional role of APP in CHT regulation in the NMJ, we went on to test whether CHT activity in the CNS is similarly affected by *APP* deficiency. We measured the CHT-mediated HACU in the brains of *APP*-null mice, *APP/APLP2* dKO mice, and their corresponding controls. The amount of HACU was determined by incubating synaptosomes prepared from the

NEUROSCIENCE

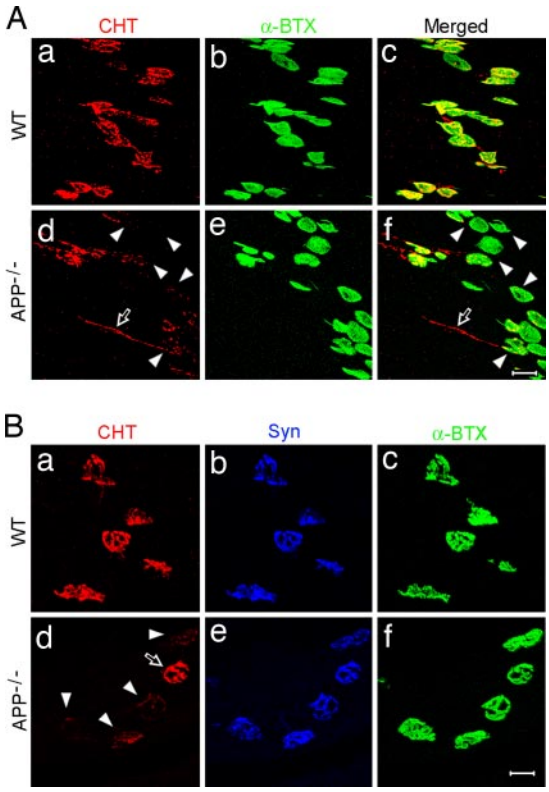

Fig. 2. Aberrant localization of CHT in the *APP*-null NMJ. (*A*) Whole-mount diaphragm muscles from littermate P0 of wild-type and *APP* KO ($APP^{-/-}$) animals were stained with anti-CHT antibody. AChR-positive postsynaptic endplates were labeled with Alexa Fluor 488-conjugated α-BTX. Open arrows mark the CHT staining beyond the endplates, and arrowheads label the synaptic sites with sparse CHT staining. The images were captured by a confocal microscope and are displayed either as individual staining or merged (last columns). (*B*) Triple labeling of the sternomastoid muscles of P18 of wild-type and $APP^{-/-}$ mice with anti-CHT antibody (CHT), anti-synaptophysin antibody (Syn), and α-BTX. Open arrow marks the synapse with normal CHT staining, and arrowheads label the synaptic sites with sparse CHT staining. (Scale bars: 20 μM.)

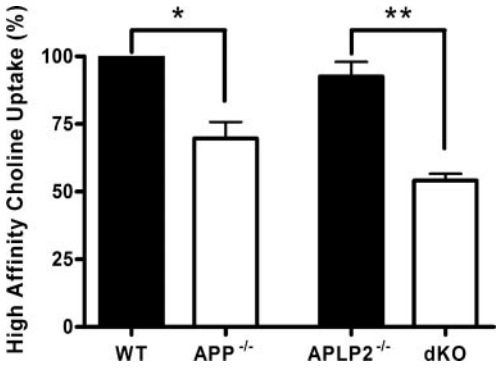

Fig. 3. Decreased HC-3-sensitive HACU in *APP* and *APP/APLP2*-null brain synaptosomes. HACU was measured in the presence and absence of 10 μM HC-3. HC-3-sensitive HACU was derived by subtracting the HC-3-insensitive value from the total uptake and normalized to that of the wild-type controls (mean ± SEM; $n = 6$; *, $P < 0.05$; **, $P < 0.01$).

forebrains of P0 mice with [^{3}H]choline in the presence or absence of 10 μM of the CHT inhibitor, HC-3. The amount of HC-3-sensitive, CHT-dependent HACU was calculated by subtracting the amount of intracellular [^{3}H]choline in the presence of HC-3 from total intracellular [^{3}H]choline (14). In *APP/APLP2* dKO mice, the HC-3-sensitive synaptosomal HACU was significantly lower than the littermate *APLP2*-null control (46% reduction; Fig. 3). Moreover, P0 *APP*-null mice also exhibited diminished HC-3-sensitive HACU (32% reduction; Fig. 3). Comparison of HACU in wild-type and *APLP2*-null mice, however, did not reveal significant differences. To establish that the impaired HACU resulting from *APP* deficiency is specifically associated with misregulation of CHT at the cholinergic projection terminals, rather than an altered CHT expression, we performed quantitative Western blotting of CHT in the striatum and spinal cord, two areas rich in cholinergic neurons. We did not detect any differences in CHT protein levels between *APP*-null samples and their corresponding wild-type controls (SI Fig. 8 *A* and *B*). Finally, to ascertain that reduced HACU is not caused by an overall defect of cholinergic neuronal function, we also performed Chat activity assays (see *SI Methods*) in the forebrains of these animals and detected no appreciable differences across all genotypes (SI Fig. 8*C*). These results indicate that the APP proteins specifically regulate CHT activity at the cholinergic synaptic terminals, and this activity applies not only to the peripheral NMJ, but also to central cholinergic neurons.

APP and CHT Interact Through the APP C-Terminal Domain. The previous studies established a physiological role of APP in regulating the localization and activity of CHT *in vivo*. To investigate the possible mechanisms for this activity, we cotransfected HEK293 cells with CHT and APP or its derivatives and performed immunoprecipitation, followed by Western blotting (Fig. 4). The results showed that full-length APP and CHT could be coimmunoprecipitated in the transfected cells (Fig. 4*A*). Transfection of the APP C-terminal fragment (APP-CTF) indicated that the interaction was mediated through the C-terminal sequences (Fig. 4*B*). Consistent with the high degree of sequence homology among the APP homologs, the APLP1 and APLP2 CTFs also could be immunoprecipitated by the anti-CHT antibody (Fig. 4*B*). This interaction appears to be specific because the CHT antibody failed to pull down a Notch CTF construct, N**Δ**E (22), or the known APP-CTF-interacting protein, FE65 (Fig. 4*B*).

APP Facilitates CHT Endocytosis. To further characterize the expression patterns of APP and CHT, we generated vectors expressing the APP-GFP or CHT-RFP fusion proteins and cotransfected these into a cholinergic cell line, SN56 (23). Examination of the fluorescence markers revealed that the majority of APP and CHT did not colocalize (Fig. 5*A*). Limited colocalization could indicate their coexpression in specific organelles or caused by nonspecific transgene overexpression.

Both APP and CHT have been shown to undergo clathrin-mediated endocytosis and localize to Rab5-positive endocytic organelles (15, 16, 24). Indeed, cotransfection of CHT-RFP (Fig. 5 *Ba–Bc*) or APP-RFP (Fig. 5 *Bd–Bf*) with a constitutively active form of Rab5-GFP revealed clear colocalization of both CHT and APP with Rab5 (Fig. 5 *Bc* and *Bf*). Based on these results, we reasoned that APP could interact with the membrane pool of CHT and regulate its endocytic recycling. Thus, we measured the rate of CHT endocytosis as a function of APP expression by using a standard biotinylation-based endocytosis assay (16). We transfected a CHT-expressing construct with an empty vector or with an APP expression vector into HEK293 cells and quantified the rates of internalization of cell surface biotin-labeled CHT protein. APP expression did not affect CHT expression because the amount of PM biotin-labeled CHT protein was similar between APP and vector-transfected cells (Fig. 5*C*, PM). However, the rate of endocytosis of CHT was significantly increased by APP expression at all time points examined (Fig. 5 *C* and *D*).

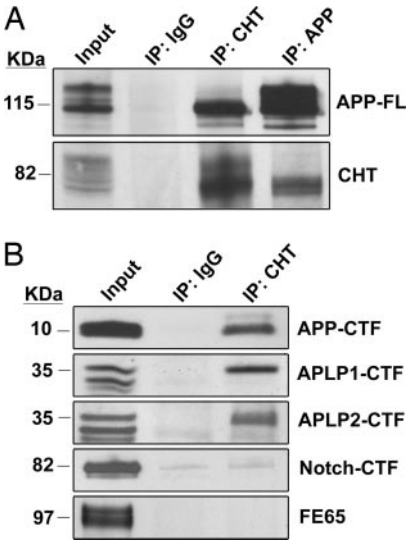

Fig. 4. Interactions of APP with CHT. (*A*) Immunoprecipitation and Western blotting (IP-WB) of HEK293 cells transfected with full-length APP (APP-FL) and CHT. Input, total protein lysate blotted with the APPC (APP) and anti-CHT (CHT) antibodies. IP using APPC (IP:APP) pulled down both APP and CHT. Likewise, anti-CHT IP (IP:CHT) pulled down both CHT and APP. IP:IgG, anti-IgG IP control. (*B*) IP-WB analysis of HEK293 cells transfected with CHT and C-terminal fragment (CTF) of APP (APP-CTF), APLP1 (APLP1-CTF), APLP2 (APLP2-CTF), Notch (Notch-CTF), and FE65, respectively. The molecular weight of APLP1-CTF and APLP2-CTF are higher than APP-CTF because they were expressed as EGFP fusion proteins.

These data suggest that APP promotes endocytic recycling of CHT molecules possibly through APP C-terminal interactions.

Discussion

We reveal here a potent and specific function of the APP family of proteins in regulating presynaptic CHT localization and activity in both central and peripheral cholinergic synapses. Loss of APP or APP/APLP2 leads to defective CHT localization in the NMJ and reduced CHT activity in the CNS. Because mice deficient in *CHT* and *APP/APLP2* share many of their neuromuscular synapse phenotypes, including defective synaptic transmission, nerve terminal sprouting, and aberrant synaptic patterning (18, 19), we postulate that misregulation of CHT is the primary cause for the NMJ defect in *APP/APLP2*-null animals. Diminished CHT capacity at the presynaptic terminals leads to impaired synaptic activity, followed by nerve sprouting and diffused pre- and postsynaptic patterning. The notion that abnormal CHT localization is not secondary to defective synaptic transmission or branch sprouting is supported by the fact that mice deficient in *Chat* display normal CHT localization despite a complete lack of synaptic activity and excessive nerve sprouting. Conversely, the NMJs of the *APP* single-null mice do not have nerve terminal sprouting, yet a clear CHT abnormality can be detected.

Gene KO studies demonstrated the important roles of Chat, CHT, and APP/APLP2 in the developing NMJ. However, the lethal phenotypes of these KO animals prevent further investigation of these molecules in mature NMJs or central cholinergic neurons. The viable phenotype and a readily detectable CHT abnormality in *APP* single-null animals offer the unique opportunity to explore these issues. Although the general NMJ morphology appears to be normal in *APP*-null mice, CHT is mistargeted in both developing and mature neuromuscular synapses. Therefore, the regulation of CHT by APP is not restricted to developing NMJ, but persists to adulthood. Interestingly, CHT localization in adult *APP*-null NMJs showed a

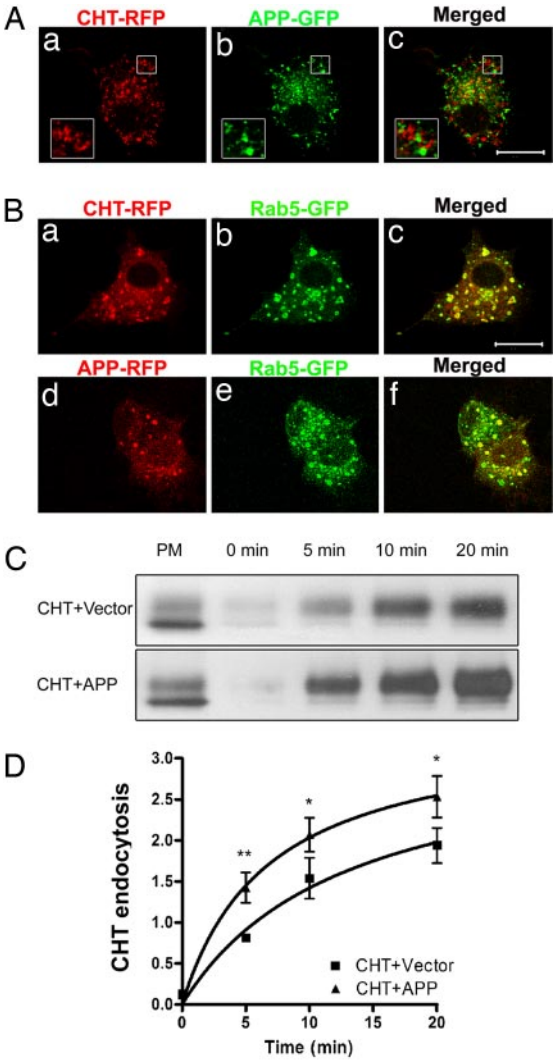

Fig. 5. APP and CHT localize to Rab5-containing endosomes and APP affects CHT endocytosis. (*A*) SN56 cells cotransfected with CHT-RFP and APP-GFP. (*Insets*) Enlarged images of the corresponding bracketed areas. (*B*) SN56 cells cotransfected with CHT-RFP and Rab5-GFP (*a–c*) or APP-RFP with Rab5-GFP (*d–f*). The images were captured by a confocal microscope and displayed either as individual fluorescence or merged (last columns). (Scale bars: 20 μM.) (*C*) Representative immunoblot of biotinylation assay of CHT internalization time course. HEK293 cells were transfected with APP or empty vector together with CHT constructs. Cell surface proteins were biotinylated, and cells were allowed to internalize at 37°C for the indicated times. (*D*) Quantitative analysis of the effects of APP on CHT internalization. Densitometric data of each time point were normalized to levels of CHT in PM. The data represent the mean ± SEM of five independent experiments. Asterisks indicate significant difference compared with the empty-vector transfected control (*, $P < 0.05$; **, $P < 0.01$, paired Student's *t* test).

greater degree of heterogeneity with reduced staining observed in a subset (≈30%) of endplates, whereas others look normal. The reason for this heterogeneity is not clear and could be attributed to the variability of individual nerves branches, which are either eliminated or expanded to occupy the entire synapse in an asynchronous manner during early postnatal NMJ maturation (21, 25). It is interesting that, although APP and APLP2 play redundant roles in CHT regulation, APP seems to exert a more dominant effect because significant CHT abnormality can only be detected in *APP*, but not *APLP2*, single-null mice. The reason for this finding is not clear and could be attributed to differences in the levels and/or patterns of expression of the two

proteins. Alternatively, APP may exhibit unique features in CHT regulation through the Aβ sequence because Bale *et al.* (26) demonstrated a direct interaction and modulation of CHT activity through Aβ in *APP* transgenic animals. The redundant and yet distinct activities of the APP family of proteins also is evident by the intriguing observation that, although *APP*/*APLP2*- and *APLP1*/*APLP2*-null mice are lethal, mice doubly deficient in *APP* and *APLP1* are viable (27).

How might the modulation of CHT activity by APP take place? Because loss of APP/APLP2 does not affect CHT protein levels, we assign APP to a step downstream of CHT protein synthesis. Blakely and colleagues (14, 28) showed that newly synthesized CHT is transported on small synaptic vesicles, which also are positive for ACh, VaChT, and synaptophysin. At presynaptic terminals, CHT mainly resides in synaptic vesicles as a reserved pool, which can undergo activity-dependent trafficking to the synaptic PM (14), followed by clathrin-mediated endocytosis (15, 16). As such, APP could in principle act on either axonal transport to control the initial pool of CHT at presynaptic terminals or synaptic PM trafficking (exocytosis) or recycling (endocytosis) of CHT, which may be tightly coupled to determine the CHT capacity and cholinergic activity.

We present the following evidence to argue against a prominent activity of APP in the axonal transport of CHT: (*i*) CHT is transported on synaptic vesicles that also are positive for VaChT. If APP is involved in the trafficking of CHT vesicles, VaChT should be simultaneously affected. However, our results clearly demonstrate a specific regulation of CHT, but not VaChT, by APP. (*ii*) Transfection of fluorescence protein-tagged APP and CHT into SN56 cells revealed a distinct expression of the two proteins in intracellular organelles and neuritic processes. Therefore, axonal trafficking of APP and CHT are likely mediated through independent processes.

CHT and VaChT are known to predominantly colocalize to synaptic vesicles at presynaptic terminals (14). However, only CHT, but not VaChT, undergoes activity-dependent synaptic PM trafficking (14), suggesting the existence of a distinct pathway that mediates the CHT membrane concentration. The preferential regulation of CHT, but not VaChT, by APP prompted us to hypothesize that APP acts on this VaChT-free pool of CHT by controlling the membrane trafficking (exocytosis) or recycling (endocytosis) of CHT, and by this means dynamically regulates the CHT density at the synaptic PM and cholinergic neurotransmission. An active role of APP in CHT endocytosis is supported by the colocalization of APP and CHT in Rab5-containing endosomal compartments and by our biotinylation experiments, which revealed a positive regulation of APP in CHT endocytosis. By extension, the absence of APP/APLP2 may lead to a retarded CHT endocytic recycling process and a defective overall dynamic regulation of CHT membrane capacity. We postulate that this regulation is mediated, at least in part, by the interactions of these two proteins through the conserved APP C-terminal domain. How this endocytic regulation affects the overall presynaptic CHT localization is not clear at present. One possible explanation is that proper dynamic regulation of membrane trafficking and endocytosis of CHT is not only required for CHT activity, but also necessary to maintain the reserved CHT pool at the nerve terminals. Although our experiments documented that APP and CHT can interact, we do not have direct proof that such protein–protein interactions occur *in vivo* under physiological conditions or that they play a functional role in APP-CHT regulation.

Although the accumulation of Aβ plaques and neurofibrillary tangles are the pathological hallmarks of AD, impaired synaptic activities, in particular cholinergic neurotransmission, are known to contribute to clinical symptoms. Whereas a direct role of CHT in AD has not been established, there is evidence for an increased CHT-dependent HC-3 binding in the cerebral cortex of AD brains (29). This finding could be mediated by the compensatory up-regulation of the CHT activity in remaining surviving cholinergic neurons, a mechanism that has been shown to operate in *Chat* and *CHT* heterozygous animals (19, 30). Cholinergic impairment has been reported to manifest at the early stages before amyloid pathology in *APP* overexpression mouse models (26, 31), supporting a role for soluble Aβ in cholinergic neuronal toxicity. A direct interpretation of Aβ in cholinergic derangement may be complicated by the confounding effect of *APP* overexpression in these animals because our data demonstrate a physiological role of APP in cholinergic regulation through CHT. These issues can be addressed by crossing the *APP* transgenic animals with *BACE1* KO mice to block Aβ production (32) or assessing the cholinergic phenotypes in *APP* knockin mice in the absence of transgene overexpression (33)

In summary, we reveal here a critical role of the APP family proteins in regulating the localization and function of the CHT in both the NMJ and central cholinergic neurons. Our studies support a model in which APP controls CHT availability at the synaptic PM by regulating the endocytic recycling of CHT through protein–protein interactions. Because CHT-mediated HACU is the rate-limiting step in cholinergic neurotransmission, and because impairment of cholinergic neurons is a cardinal feature of AD pathogenesis, our findings not only uncover a unique activity of APP in cholinergic neurons, but also have important implications in understanding the pathogenic mechanisms of AD.

Methods

Reagents and Animals. CHT was amplified from a mouse brain cDNA library by PCR and cloned into the pEGFP-N1 expression vector with GFP tagged at the C terminus of CHT. Human APP695 was cloned into pcDNA3.1 vector. APP-CTF was generated by fusing the APP signal peptide with the C-terminal fragment starting from Aβ. APLP1-CTF and APLP2-CTF were generated by fusing the APP signal peptide with the corresponding APLP1 and APLP2 C-terminal fragments into the pEGFP-N1 expression vector. Notch-CTF (N**Δ**E) and Rab5-GFP constructs were previously described (22, 34). The antibodies used in this study were anti-synaptophysin (DAKO, Carpinteria, CA), anti-CHT (Chemicon International, Temecula, CA), anti-VaCHT (Synaptic Systems, Goettingen, Germany), 4G8 (Signet Laboratories, Dedham, MA), and APPC (35). Alexa Fluor-conjugated secondary antibodies and α- BTX were purchased from Molecular Probes (Eugene, OR).

The *APP* and *APLP2* KO mice were described previously (18, 36, 37). These mice were backcrossed to a C57BL/6J background for at least 10 generations. All animal experiments were performed in accordance with the Baylor College of Medicine Institutional Animal Care and Use Committee and with national regulations and policies. Whole-mount staining of the diaphragm muscle was performed as previously described (18). The images presented represent single-projected images derived from overlaying each set of *Z* images. The quantitation of colocalization was done by using the Image J program from the National Institutes of Health.

Synaptosomal Choline Transport Assay. Mouse brain synaptosomal preparations were performed as previously described (38). Fifty micrograms of the synaptosomal protein was incubated for 15 min at 37°C in the presence or absence of 10 μM HC-3. Choline transport was initiated by the addition of 50 μl of 100 nM [^{3}H]choline [83 Ci/mmol (1 Ci = 37 GBq); GE Healthcare, Chalfont St. Giles, U.K.], and the incubation was continued for 5 min at 37°C. The reaction was stopped by adding 1 ml of ice-cold KRH buffer containing 1 mM HC-3. Pellets were lysed in 1% SDS, 0.2 mM NaOH, and radioactivity measured with a liquid scintillation counter (LS 600IC; Beckman Instruments, Columbia, MD). The assays were performed in triplicate, and

data were normalized by protein content. Specific CHT-mediated HC-3-sensitive HACU was defined as total choline uptake minus choline uptake in the presence of HC-3.

Cell Culture. HEK293 and SN56 cells were grown in DMEM containing 10% FBS. These cells were transiently transfected with cDNA expression constructs on coverslips. After transfection, SN56 cells were differentiated in serum-free medium supplemented with 1 mM dibutyryl-cAMP (Sigma–Aldrich, St. Louis, MO) for 2 days. The cells were fixed in buffered 4% paraformaldehyde, and images were captured by an Axioskop2 confocal microscope (Zeiss, Thornwood, NY).

Biotinylation Assay. The HEK293 cells were transiently cotransfected with CHT and empty vector or CHT with APP. Cells were washed with ice-cold PBS and treated with 1.5 mg/ml sulfo-NHS-SS-biotin (Pierce, Rockford, IL) for 1 h. Biotinylating reagents were removed by incubating with 100 mM cold glycine, followed by three washes with cold PBS/Ca-Mg. Cells were incubated at 37°C to allow internalization to occur, which was subsequently terminated by transferring culture plates to ice. Residual cell-surface biotin was then stripped by incubating cells once for 15 min and twice for 30 min with freshly prepared 50 mM mercaptoethanesulfonic acid in TE buffer [150 mM NaCl/1 mM EDTA/0.2% BSA/20 mM Tris (pH 8.6)]. Cells were then lysed in 1% CHAPS buffer containing protease inhibitors (Roche Diagnostics, Indianapolis, IN). Biotinylated and nonbiotinylated proteins were separated by incubation with Ultralink-Neutravidin bead (Pierce). CHT internalization was calculated as the percentage of total PM CHT levels.

We thank N. Aithmitti and X. Chen for expert technical assistance; members of the H.Z. laboratory for discussion; R. Atkinson and the Mental Retardation and Developmental Disabilities Research Center at Baylor College of Medicine for confocal imaging support; Dr. K.-F. Lee (Salk Institute, La Jolla, CA) for Chat KO embryos; B. Knoll (University of Houston, Houston, TX) and R. Kopan (Washington University, St. Louis, MO) for Rab5 and Notch constructs, respectively; and B. Wainer (Emory University, Atlanta, GA) for SN56 cells. This work was supported by National Institutes of Health Grants NS40039, AG20670, and AG21141 and Alzheimer's Association Grants ZEN-03-4757 and IIRG-06-25779. B.W. was supported by National Institutes of Health Training Grant T32 AG000183.

1. Rovelet-Lecrux A, Hannequin D, Raux G, Le Meur N, Laquerriere A, Vital A, Dumanchin C, Feuillette S, Brice A, Vercelletto M, *et al*. (2006) *Nat Genet* 38:24–26.
2. Hardy J, Selkoe DJ (2002) *Science* 297:353–356.
3. Zheng H, Koo EH (2006) *Mol Neurodegener* 1:5.
4. Schubert W, Prior R, Weidemann A, Dircksen H, Multhaup G, Masters CL, Beyreuther K (1991) *Brain Res* 563:184–194.
5. Shigematsu K, McGeer PL, McGeer EG (1992) *Brain Res* 592:353–357.
6. Koo EH, Sisodia SS, Archer DR, Martin LJ, Weidemann A, Beyreuther K, Fischer P, Masters CL, Price DL (1990) *Proc Natl Acad Sci USA* 87:1561–1565.
7. Sisodia SS, Koo EH, Hoffman PN, Perry G, Price DL (1993) *J Neurosci* 13:3136–3142.
8. Yamazaki T, Selkoe DJ, Koo EH (1995) *J Cell Biol* 129:431–442.
9. Satpute-Krishnan P, Degiorgis JA, Conley MP, Jang M, Bearer EL (2006) *Proc Natl Acad Sci USA* 103:16532–16537.
10. McKinney M, Coyle JT, Hedreen JC (1983) *J Comp Neurol* 217:103–121.
11. Edeline JM (1999) *Prog Neurobiol* 57:165–224.
12. Kilgard M (2003) *Neuron* 38:678–680.
13. Sarter M, Parikh V (2005) *Nat Rev Neurosci* 6:48–56.
14. Ferguson SM, Savchenko V, Apparsundaram S, Zwick M, Wright J, Heilman CJ, Yi H, Levey AI, Blakely RD (2003) *J Neurosci* 23:9697–9709.
15. Ribeiro FM, Alves-Silva J, Volknandt W, Martins-Silva C, Mahmud H, Wilhelm A, Gomez MV, Rylett RJ, Ferguson SS, Prado VF, Prado MA (2003) *J Neurochem* 87:136–146.
16. Ribeiro FM, Black SA, Cregan SP, Prado VF, Prado MA, Rylett RJ, Ferguson SS (2005) *J Neurochem* 94:86–96.
17. Sanes JR, Lichtman JW (1999) *Annu Rev Neurosci* 22:389–442.
18. Wang P, Yang G, Mosier DR, Chang P, Zaidi T, Gong YD, Zhao NM, Dominguez B, Lee KF, Gan WB, Zheng H (2005) *J Neurosci* 25:1219–1225.
19. Ferguson SM, Bazalakova M, Savchenko V, Tapia JC, Wright J, Blakely RD (2004) *Proc Natl Acad Sci USA* 101:8762–8767.
20. Brandon EP, Lin W, D'Amour KA, Pizzo DP, Dominguez B, Sugiura Y, Thode S, Ko CP, Thal LJ, Gage FH, Lee KF (2003) *J Neurosci* 23:539–549.
21. Keller-Peck CR, Walsh MK, Gan WB, Feng G, Sanes JR, Lichtman JW (2001) *Neuron* 31:381–394.
22. Schroeter EH, Kisslinger JA, Kopan R (1998) *Nature* 393:382–386.
23. Hammond DN, Wainer BH, Tonsgard JH, Heller A (1986) *Science* 234:1237–1240.
24. Sabo SL, Ikin AF, Buxbaum JD, Greengard P (2003) *J Neurosci* 23:5407–5415.
25. Walsh MK, Lichtman JW (2003) *Neuron* 37:67–73.
26. Bales KR, Tzavara ET, Wu S, Wade MR, Bymaster FP, Paul SM, Nomikos GG (2006) *J Clin Invest* 116:825–832.
27. Heber S, Herms J, Gajic V, Hainfellner J, Aguzzi A, Rulicke T, von Kretzschmar H, von Koch C, Sisodia S, Tremml P, *et al*. (2000) *J Neurosci* 20:7951–7963.
28. Matthies DS, Fleming PA, Wilkes DM, Blakely RD (2006) *J Neurosci* 26:6200–6212.
29. Slotkin TA, Nemeroff CB, Bissette G, Seidler FJ (1994) *J Clin Invest* 94:696–702.
30. Brandon EP, Mellott T, Pizzo DP, Coufal N, D'Amour KA, Gobeske K, Lortie M, Lopez-Coviella I, Berse B, Thal LJ, *et al*. (2004) *J Neurosci* 24:5459–5466.
31. Stokin GB, Lillo C, Falzone TL, Brusch RG, Rockenstein E, Mount SL, Raman R, Davies P, Masliah E, Williams DS, Goldstein LS (2005) *Science* 307:1282–1288.
32. Ohno M, Sametsky EA, Younkin LH, Oakley H, Younkin SG, Citron M, Vassar R, Disterhoft JF (2004) *Neuron* 41:27–33.
33. Hartmann J, Erb C, Ebert U, Baumann KH, Popp A, Konig G, Klein J (2004) *Neuroscience* 125:1009–1017.
34. Rosenfeld JL, Moore RH, Zimmer KP, Alpizar-Foster E, Dai W, Zarka MN, Knoll BJ (2001) *J Cell Sci* 114:4499–4508.
35. Xia X, Wang P, Sun X, Soriano S, Shum WK, Yamaguchi H, Trumbauer ME, Takashima A, Koo EH, Zheng H (2002) *Proc Natl Acad Sci USA* 99:8760–8765.
36. Zheng H, Jiang M, Trumbauer ME, Sirinathsinghji DJ, Hopkins R, Smith DW, Heavens RP, Dawson GR, Boyce S, Conner MW, *et al*. (1995) *Cell* 81:525–531.
37. von Koch CS, Zheng H, Chen H, Trumbauer M, Thinakaran G, van der Ploeg LH, Price DL, Sisodia SS (1997) *Neurobiol Aging* 18:661–669.
38. Janz R, Hofmann K, Sudhof TC (1998) *J Neurosci* 18:9269–9281.